MORPHOLOGICAL ANALYSIS AND CLASSIFICATION VIA CONVEX HULL OF 3D SPECT IMAGE

R. Helm, J.Kukal, A. Prochazka

DCCE FCHE ICT Prague

Abstract

The space reconstruction of SPECT pictures is producing a 3D array of nonnegative intensities, which is subject of morphological analysis. After all steps of 3D image processing the 3D binary image can be investigated directly or after the morphological transforms. The different properties of original binary image, its convex hull and deficit enable us to construct a set of descriptors. These descriptors were used for the pattern realization. The erosion and dilation enabled to estimate region surface and then realize radial characteristics based on digital volume, surface, maximum internal sphere and diameter. Our methodology is based on the variation of relative threshold together with relative pre-erosion. The results were converted to the relative logarithmic form and the linear model of single neuron was used for the classification of brain disease.

1 Introduction

The 3D Single Proton Emission Computer Tomography (SPECT) with ^{19}F-glucose tracer is a method for the monitoring of human brain structure and activities. It can be used for determination of some brain disease like - Alzheimer disease.

For classification of these pictures can be used methods of digital morphology. Digital morphology is based on the theoretical background of mathematical morphology and it enables us to study details in binary images. The morphological transforms are non-linear ones.

2 Radial approach to digital morphology

The radius ρ of maximum internal sphere is a trivial radial characteristic. The second radial characteristics can be formed from the maximum point distance as $r_{\max} = d_{\max}/2$. The third radial characteristic can be derived from the domain volume. Intuitively, we find the radius of sphere with the same volume as the domain. From the famous formula

$$V = \frac{4}{3}\pi r^3 \tag{1}$$

we directly obtain

$$r_{\mathrm{vol}} = \sqrt[3]{\frac{3\mathrm{V}(\boldsymbol{X})}{4\pi}} \tag{2}$$

as another radial characteristic. The surface area estimate is not too accurate but we can also find a sphere with the same surface area as the domain. From the formula $S = 4\pi r^2$ we obtain another radial descriptor

$$r_{\mathrm{surf}} = \sqrt{\frac{\mathrm{S}(\boldsymbol{X})}{4\pi}} \tag{3}$$

There is also a habit to use an effective radius

$$r_{\mathrm{eff}} = \frac{3\mathrm{V}(\boldsymbol{X})}{\mathrm{S}(\boldsymbol{X})} \tag{4}$$

in many technical applications. The main advantage of radial approach to the morphological classification is in the relationship $\rho = r_{\mathrm{max}} = r_{\mathrm{vol}} = r_{\mathrm{surf}} = r_{\mathrm{eff}} = r$ which holds just for the spherical domain of radius r. Anyway, the radii are not completely equal each other. Convex hull of any 3D set can be also studied in the terms of radii. Adequate radii of convex hull can be denoted as $\rho^*, r^*_{\mathrm{max}}, r^*_{\mathrm{vol}}, r^*_{\mathrm{surf}}, r^*_{\mathrm{eff}}$. They are equal to the original values $\rho, r_{\mathrm{max}}, r_{\mathrm{vol}}, r_{\mathrm{surf}}, r_{\mathrm{eff}}$ for any convex set.

3 Invariant morphological description and classification of 3D image

All the morphological descriptors are invariant to translation and rotation. But they are not scaling invariant. It is useful to introduce their ratios or rather logarithms of their ratios to obtain the scaling invariance. So, the final system is TSR invariant, which is amusing property. Eight ratios form the pattern $\boldsymbol{p} = (\rho / r^*_{\mathrm{vol}}, r_{\mathrm{max}} / r^*_{\mathrm{vol}}, r_{\mathrm{vol}} / r^*_{\mathrm{vol}}, r_{\mathrm{surf}} / r^*_{\mathrm{vol}}, r_{\mathrm{eff}} / r^*_{\mathrm{vol}}, \rho^* / r^*_{\mathrm{vol}}, r^*_{\mathrm{surf}} / r^*_{\mathrm{vol}}, r^*_{\mathrm{eff}} / r^*_{\mathrm{vol}}) \in \mathbf{R}^8_+$

Their natural logarithms can extend them and form alternative pattern $\boldsymbol{x} = (\boldsymbol{p}, \log \boldsymbol{p})$.

The logarithmic pattern can be passed on the inputs of artificial neuron, artificial neural network or any decision system. Bipolar perceptron, sigmoid neuron, MLP, RBF or SOM ANNs are good models of classification engine. In our case we apply bipolar perceptron model to obtain binary classifier with single output. The model of bipolar perceptron is based on linear combination of given signals and sign nonlinearity as

$$y = \mathrm{sgn}\left(\sum\nolimits_{k=0}^{n} w_k x_k\right) \text{ with } x_0 = 1 \tag{5}$$

4 Biomedical application: AD classification from 3D SPECT brain image

A collection of 25 patients and their 3D SPECT scans of brain were split into three groups:

- AD – Alzheimer disease (11 patients)
- CN – Control normal (8 patients)
- CD – Control diseased (6 patients)

A pattern $\boldsymbol{x}$ of size 16 was formed from radius ratios and their natural logarithms as described above. The classification task was oriented to the classification of AD group against union of CN and CD group. Our aim was to realize AD classifier with the sensitivity and specificity higher than 0.9. It means one positive and one negative error at most in our case. Several items were not useful for the classification. We reduced the number of ANN inputs to seven only. Our study was effective only for threshold $\theta = 0.7 I_{\mathrm{max}}$ (active brain contours) and threshold $\theta = 0.9 I_{\mathrm{max}}$ (cerebellum contours only).

The adequate formulas are

$$AD_{0.7} = \mathrm{sgn}\begin{pmatrix} -0.4305 + 0.0013\, r_{\mathrm{eff}} / r^*_{\mathrm{vol}} - 0.0012\, r_{\mathrm{surf}} / r^*_{\mathrm{vol}} \\ + 0.0012\, r_{\mathrm{max}} / r^*_{\mathrm{vol}} - 0.1902\, r^*_{\mathrm{eff}} / r^*_{\mathrm{vol}} + 0.6192\, r^*_{\mathrm{surf}} / r^*_{\mathrm{vol}} \\ + 0.0003 \log(r_{\mathrm{vol}} / r^*_{\mathrm{vol}}) - \log(r^*_{\mathrm{surf}} / r^*_{\mathrm{vol}}) \end{pmatrix} \tag{6}$$

$$AD_{0.9} = \operatorname{sgn}\begin{pmatrix} 0.2579 + 0.4382\ \rho / r^{*}_{\mathrm{vol}} - r_{\mathrm{vol}} / r^{*}_{\mathrm{vol}} + 0.3941\ r_{\mathrm{surf}} / r^{*}_{\mathrm{vol}} \\ -\ 0.1269 \log(\rho / r^{*}_{\mathrm{vol}}) + 0.6017 \log(r_{\mathrm{vol}} / r^{*}_{\mathrm{vol}}) \\ -0.3831 \log(r_{\mathrm{surf}} / r^{*}_{\mathrm{vol}}) - 0.0611 \log(r^{*}_{\max} / r^{*}_{\mathrm{vol}}) \end{pmatrix} \tag{7}$$

Both formulas have sensitivity 10/11 and specificity 13/14 which is higher than 0.9. but the first formula for contour threshold $\theta = 0.7 I_{\max}$ is more clear for the biomedical interpretation.

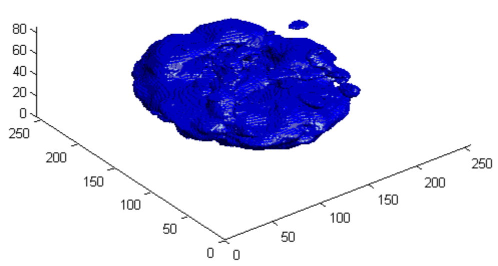

Fig. 1: Scan of CN brain for $\theta = 0.5 I_{\max}$

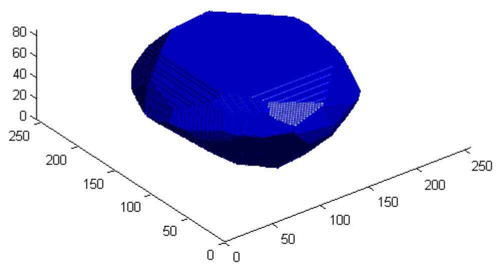

Fig. 2: Convex hull of CN brain for $\theta = 0.5 I_{\max}$

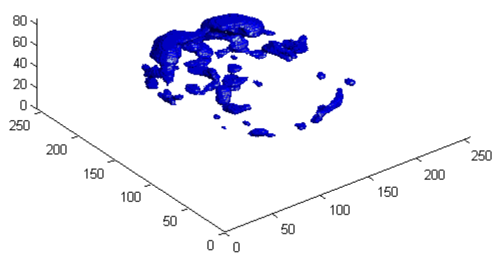

Fig. 3: Scan of CN brain for $\theta = 0.7 I_{\max}$

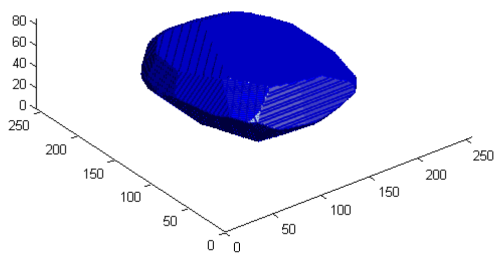

Fig. 4: Convex hull of CN brain for $\theta = 0.7 I_{\max}$

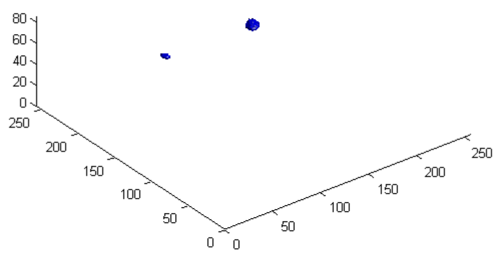

Fig. 5: Scan of CN brain for $\theta = 0.9 I_{\max}$

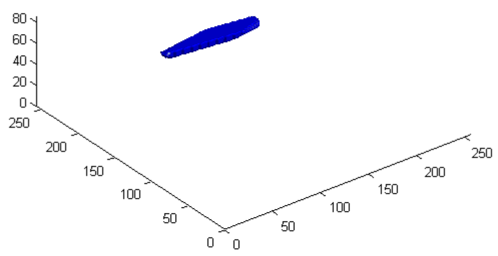

Fig. 6: Convex hull of CN brain for $\theta = 0.9 I_{\max}$

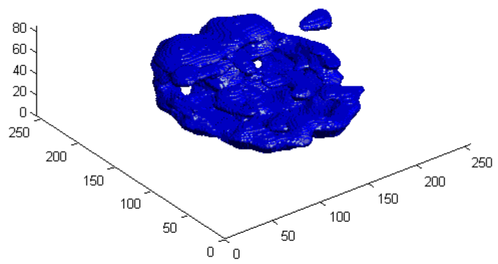

Fig. 7: Scan of AD brain for $\theta = 0.5I_{\max}$

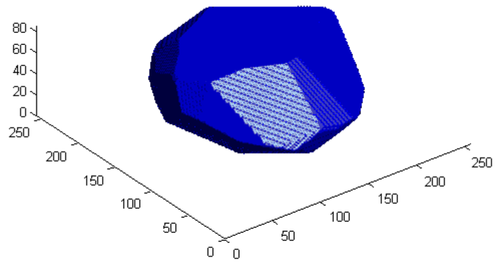

Fig. 8: Convex hull of AD brain for $\theta = 0.5I_{\max}$

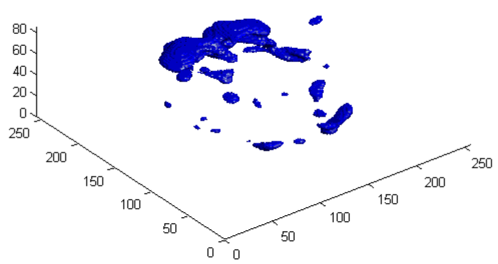

Fig. 9: Scan of AD brain for $\theta = 0.7I_{\max}$

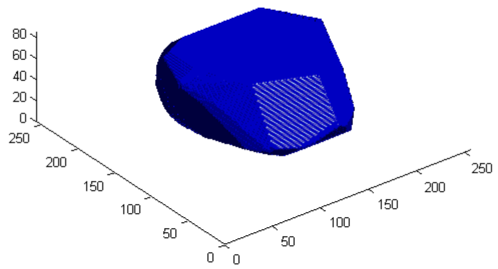

Fig.10: Convex hull of AD brain for $\theta = 0.7I_{\max}$

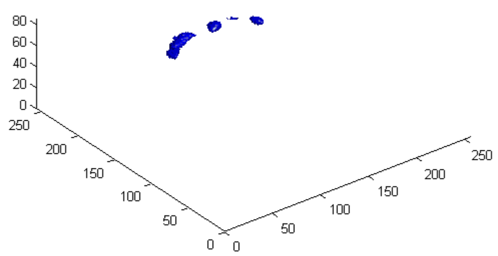

Fig.11: Scan of AD brain for $\theta = 0.9I_{\max}$

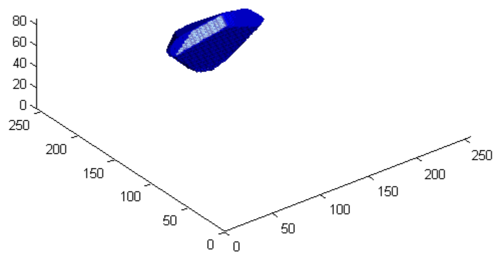

Fig.12: Convex hull of AD brain for $\theta = 0.9I_{\max}$

Acknowledgement

This work has been supported by the Ministry of Education of the Czech Republic MSM 6046137306.

References

[1] HLAVÁČ, V.; SEDLÁČEK, M. 2000. *Zpracování signálů a obrazů*. Praha : Vydavatelství ČVUT, 2002. ISBN 80-01-02114-9.